

# Parallel Split Learning with Global Sampling

Mohammad Kohankhaki<sup>1</sup>, Ahmad Ayad<sup>2</sup>, Mahdi Barhoush<sup>3</sup>, and Anke Schmeink<sup>4</sup>

Chair of Information Theory and Data Analytics

RWTH Aachen University, D-52074 Aachen, Germany

Email: <sup>1,2,3,4</sup>{mohammad.kohankhaki, ahmad.ayad, mahdi.barhoush, anke.schmeink}@inda.rwth-aachen.de

**Abstract**—Distributed deep learning in resource-constrained environments faces scalability and generalization challenges due to large effective batch sizes and non-identically distributed client data. We introduce a server-driven sampling strategy that maintains a fixed global batch size by dynamically adjusting client-side batch sizes. This decouples the effective batch size from the number of participating devices and ensures that global batches better reflect the overall data distribution. Using standard concentration bounds, we establish tighter deviation guarantees compared to existing approaches. Empirical results on a benchmark dataset confirm that the proposed method improves model accuracy, training efficiency, and convergence stability, offering a scalable solution for learning at the network edge.

**Index Terms**—Parallel split learning, distributed deep learning, non-iid data, IoT.

## I. INTRODUCTION

Distributed deep learning (DDL) has emerged as a powerful paradigm in the era of the Internet of Things (IoT), addressing the challenges posed by the proliferation of resource-constrained devices and the exponential growth of data at the network edge [1]–[3]. Split learning (SL) [4], [5] is a DDL paradigm designed for environments with constrained computational and communication resources, such as IoT settings. In SL, neural network training is partitioned between client devices and a central server. This setup enhances data privacy, minimizes client-side computation, and facilitates faster convergence [4], [6], [7]. However, the sequential execution across devices introduces considerable training and communication latency [6].

To address training latency in SL, parallel split learning (PSL) [8]–[12] has been proposed and introduces parallelism without the need for multiple server model instances like in split federated learning (v1) [13] or client model aggregation like in FedAvg [14]. However, PSL encounters the *large effective batch size problem* [11], [15], where the effective batch size scales with the number of clients. Additionally, devices usually contribute from local datasets that are not independent and identically distributed (IID) and vary in sizes, causing batch distributions to deviate from the overall data distribution, which can lead to poor generalization. This issue of *non-IID data* is a general problem in DDL, not specific to PSL.

We propose *parallel split learning with global sampling* (GPSL) building upon the original PSL framework introduced in [8] to address the large effective batch size problem and the issue of non-IID data. GPSL allows for variable local batch sizes that sum up to a fixed global batch size. This

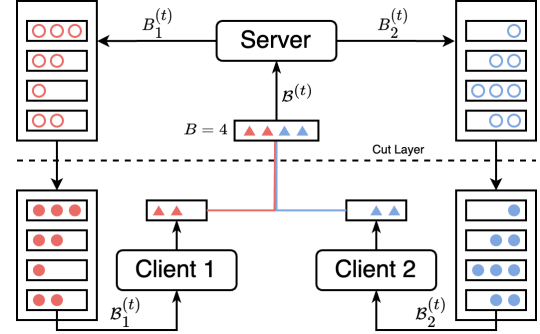


Fig. 1. Schematic illustration of the proposed GPSL method with variable local batch sizes summing to a fixed global batch size, mitigating the large effective batch size and non-IID data problems in PSL.

decouples the number of clients from the effective batch size. We show that this decoupling is crucial for controlling the deviation probability of global batches from the overall data distribution, leading to improved model performance and reduced training latency in non-IID settings. In particular, we show that the choice of local batch sizes is crucial for controlling the deviation probability. An overview of GPSL is shown in Figure 1. The main contributions of this paper are listed below:

- We introduce the GPSL method to address the large effective batch size problem and the non-IID data problem in PSL.
- We analyze the global batch deviation and establish tight deviation bounds for GPSL.
- Our simulation results show that GPSL reduces the deviation probability of global batches significantly, leading to improved accuracy and reducing training latency.

The remainder of this paper is organized as follows. Sections II and III present related works and preliminaries of our work. In Section IV, we introduce our novel GPSL method and analyze the deviation probability of global batches. Section V presents the simulation results and addresses known limitations. Section VI concludes the paper with final remarks. Code and results available on GitHub [16].

## II. RELATED WORK

Jeon and Kim [8] introduce PSL and use gradient averaging over all clients to address the client decoupling problem, where the information flow between clients is decoupled during BP. They fixed the local batch sizes proportional to the dataset size

of each client. Lyu et al. [17] propose averaging the clients' local loss function outputs instead of their local gradients. This approach aligns with that of [8] due to the linearity of the gradient operator, but enhances privacy as clients can compute the local loss functions without sharing labels. Both show stable convergence and improved accuracy in both IID and non-IID settings. However, the proportion of each client's data in the total was chosen to yield an integer when scaled by the global batch size to determine local batch sizes. In practice, rounding is typically necessary when determining each client's local batch size, which can lead to imbalances in the global batch composition. Furthermore, the large effective batch size problem is not addressed in these works.

To mitigate the large effective batch size problem, Pal et al. [15] propose scaling the learning rate on the server side while keeping the local batch size fixed and identical for all clients. Following the line of work from [12], Oh et al. [11] propose using smashed data augmentation, local loss function design and FedAvg for the client models to overcome the large effective batch size problem and client model decoupling. Pal et al. [15] and Oh et al. [11] assume that the effective batch size scales with the number of clients. However, it has been shown that increasing the batch size leads to diminishing returns for gradient estimation [18] and that smaller batch sizes [19] can be more beneficial for model generalization, if communication constraints allow. Furthermore, the empirical results are reported only for IID settings.

Cai and Wei [20] propose an incentive mechanism to handle non-IID data in PSL, which encourages clients with larger and more evenly distributed datasets to participate in training. The bargaining game approach for personalized SL [21] balances energy consumption and privacy in non-IID settings. However, these methods may face scalability issues and may not fully address the heterogeneity of data distributions across diverse clients.

### III. PRELIMINARIES

We consider the PSL setting from [8]. The client index set is  $\mathcal{K} = \{1, 2, \dots, K\}$ . A server and  $|\mathcal{K}| = K$  clients train a neural network model with parameter vector  $\mathbf{w}$  collaboratively using the PSL framework. We focus on supervised classification tasks, where the dataset  $\mathcal{D}_k$  of each client  $k \in \mathcal{K}$  consists of input-label pairs  $\mathcal{D}_k = \{(\mathbf{x}_{k,i}, y_{k,i})\}_{i=1}^{D_k}$ , where  $D_k \in \mathbb{N}$  is the dataset size,  $\mathbf{x}_{k,i}$  is the input data, and  $y_{k,i} \in \mathcal{M}$  is the ground truth class label of  $\mathbf{x}_{k,i}$ . Here,  $\mathcal{M} = \{1, 2, \dots, M\}$  represents all classes and  $M \in \mathbb{N}$  is the number of classes. The overall dataset  $\mathcal{D}_0 = \bigcup_{k \in \mathcal{K}} \mathcal{D}_k$  is the union of all clients' datasets, with a total size  $D_0 = \sum_{k \in \mathcal{K}} D_k$ .

The *class distribution* of a client  $k$  with class label vector  $\mathbf{y}_k \in \mathcal{M}^{D_k}$  is denoted as  $\beta_k \in \mathbb{R}^M$  with

$$\beta_k = \frac{1}{D_k} (c(\mathbf{y}_k, 1), c(\mathbf{y}_k, 2), \dots, c(\mathbf{y}_k, M))^\top,$$

where  $c(\mathbf{y}, m)$  counts the number of times class  $m$  appears in  $\mathbf{y}$ . The *overall class distribution* of  $\mathcal{D}_0$  with class label vector  $\mathbf{y}_0 \in \mathcal{M}^{D_0}$  is denoted as  $\beta_0 \in \mathbb{R}^M$  according to the same definition.

Every epoch consists of  $T \in \mathbb{N}$  optimization steps. The set of optimization steps is denoted as  $\mathcal{T} = \{1, 2, \dots, T\}$ . Each client  $k$  has a *local batch size*  $B_k^{(t)} \in \mathbb{N}$ . The *global batch size*  $B^{(t)} = \sum_{k \in \mathcal{K}} B_k^{(t)}$  is the total number of intermediate representations that arrive at the server in each optimization step  $t \in \mathcal{T}$ . Accordingly, we differentiate between local batches  $\mathcal{B}_k^{(t)} \subseteq \mathcal{D}_k$  and the global batch  $\mathcal{B}^{(t)} = \bigcup_{k \in \mathcal{K}} \mathcal{B}_k^{(t)}$ .

PSL splits the model into client-side parameters  $\mathbf{w}_c$  and server-side parameters  $\mathbf{w}_s$ . Before training, the server sends  $\mathbf{w}_c$  to the clients, each storing a copy  $\mathbf{w}_{c,k}$  with identical initial values. Accordingly, the model function  $f(\mathbf{x}; \mathbf{w})$  is split into two functions  $f_c$  and  $f_s$  as  $f(\mathbf{x}; \mathbf{w}) = f_s(f_c(\mathbf{x}; \mathbf{w}_c); \mathbf{w}_s)$ . The goal is to find the optimal model parameters  $\mathbf{w}^* = (\mathbf{w}_s^*, \mathbf{w}_c^*)^\top$  that minimize the global loss function. Each optimization step  $t \in \mathcal{T}$  involves the following substeps:

- 1) **Parallel Client-Side Forward Propagation (FP):** Each client  $k$  samples a local batch  $\mathcal{B}_k^{(t)} \subseteq \mathcal{D}_k$  with a local batch size of  $B_k^{(t)}$  and sends  $f_c(\mathcal{B}_k^{(t)}; \mathbf{w}_{c,k})$  with the corresponding labels to the server.
- 2) **Server-Side FP:** The server concatenates the received activations to obtain the global batch  $\mathcal{B}^{(t)} = \bigcup_{k \in \mathcal{K}} \mathcal{B}_k^{(t)}$  and computes the final predictions  $f_s(\mathcal{B}^{(t)}; \mathbf{w}_s)$  to compute the average loss.
- 3) **Server-Side Backward Propagation (BP):** The server computes the server-gradients through backpropagation, updates its model parameters according to the optimization algorithm, and sends the gradient of the first server-side layer (*cut layer*) to all clients.
- 4) **Parallel Client-Side BP:** Each client  $k$  continues back-propagation using the cut layer gradient to compute the client-gradients  $\mathbf{g}_{\mathbf{w}_{c,k}}^{(t)}$  and sends it back to the server.
- 5) **Server-Side Gradient Averaging:** The server computes the average client gradients  $\bar{\mathbf{g}}_{\mathbf{w}_c}^{(t)} = \sum_{k \in \mathcal{K}} \frac{D_k}{D_0} \mathbf{g}_{\mathbf{w}_{c,k}}^{(t)}$  and sends it to all clients.
- 6) **Parallel Client-Side Model Update:** Each client uses  $\bar{\mathbf{g}}_{\mathbf{w}_c}^{(t)}$  to update its model parameters.

An epoch is concluded after  $T$  optimization steps.  $T$  is determined by the number of non-empty global batches that can be formed from the clients' datasets until depletion and thus depends on the sampling procedure. The model is trained for a fixed number of epochs  $E \in \mathbb{N}$ .

### IV. SYSTEM MODEL

This section introduces the proposed GPSL method and analyzes how it improves the alignment between global batches and the overall data distribution compared to random uniform sampling in a centralized setting.

#### A. Parallel Split Learning with Global Sampling

In GPSL, we replace the notion of fixed per-client batch sizes with a single *global batch size*  $B$ . The server first gathers each client's dataset size  $D_k$ . This information can trivially be obtained from the server through counting the number of samples that arrive from each client and is not sensitive. Before

training the server must choose how many samples  $B_k^{(t)}$  each client  $k$  will contribute to each training step  $t \in \mathcal{T}$ , subject to

$$\sum_{k \in \mathcal{K}} B_k^{(t)} = B.$$

Rather than uniformly fixing these  $B_k^{(t)}$ , we draw the local batch sizes using a global sampling procedure over the pooled data. We first set each client's remaining dataset size  $D_k^{(0)} = D_k$ . Then, for each  $t \in \mathcal{T}$ :

- 1) **Dynamic Sampling.** For  $i = 1, \dots, B$ :
  - a) Compute *client weights*

$$\pi_k^{(i)} = D_k^{(i)} / \sum_{j \in \mathcal{K}} D_j^{(i)}.$$

- b) Sample a client index  $z_i \sim \text{Categorical}(\boldsymbol{\pi}^{(i)})$ .
- c) Decrement its remaining dataset size:

$$D_{z_i}^{(i+1)} \leftarrow D_{z_i}^{(i)} - 1.$$

- 2) **Batch Composition.** After  $B$  draws, the number of samples from client  $k$  are obtained by

$$B_k^{(t)} = |\{i : z_i = k\}|$$

Remaining dataset sizes are reset to  $D_k^{(0)} = D_k^{(i)}$

The server forwards the  $\{B_k^{(t)}\}_{t \in \mathcal{T}}$  to each client before training starts. During training clients uniformly sample random mini-batches using  $B_k^{(t)}$  as local batch size. Because each draw in step 1) selects one of the remaining points uniformly without replacement, the resulting batch during training is *exactly* a uniform draw at random of  $B$  distinct samples from the union  $\mathcal{D}_0$ . The rest of the PSL training loop remains unchanged, allowing seamless integration of the sampling procedure into existing PSL frameworks.

### B. Deviation Analysis

We assess how well a batch  $\mathcal{B} \subset \mathcal{D}_0$  of size  $B$  reflects the true label distribution  $\boldsymbol{\beta}_0$  using the  $\ell_1$  deviation:

$$\Delta(\mathcal{B}, \boldsymbol{\beta}_0) = \sum_{m \in \mathcal{M}} |\hat{\beta}_m - \beta_{0,m}|, \quad \hat{\beta}_m = \frac{1}{B} c(\mathcal{B}, m).$$

where  $c(\mathcal{B}, m)$  is the count of class- $m$  samples in  $\mathcal{B}$ . Throughout we assume

$$B \leq D_0, \quad 0 < \varepsilon \leq 1 - \frac{1}{D_0},$$

so that all finite-population corrections remain positive and  $\varepsilon B \leq B - 1$ . When  $\mathcal{B}$  is drawn by sampling  $B$  points without replacement from  $\mathcal{D}_0$ , the count  $Y_m = c(\mathcal{B}, m)$  follows a hypergeometric distribution

$$Y_m \sim \text{Hypergeometric}(D_0, c(D_0, m), B).$$

with  $\mathbb{E}[Y_m] = B \beta_{0,m}$ . By Serfling's inequality with finite-population correction [22],

$$\begin{aligned} \Pr(|Y_m - B \beta_{0,m}| \geq \varepsilon B) &= \Pr\left(\left|\frac{Y_m}{B} - \beta_{0,m}\right| \geq \varepsilon\right) \\ &\leq 2 \exp\left(-\frac{2 \varepsilon^2 B}{1 - \frac{B-1}{D_0}}\right). \end{aligned}$$

Although the  $\{Y_m\}_{m \in \mathcal{M}}$  are dependent as they are required to sum up to  $B$ , a union bound yields

$$\begin{aligned} \Pr\left(\Delta(\mathcal{B}, \boldsymbol{\beta}_0) \geq M \varepsilon\right) &\leq \sum_{m \in \mathcal{M}} 2 \exp\left(-\frac{2 \varepsilon^2 B}{1 - \frac{B-1}{D_0}}\right) \\ &= 2M \exp\left(-\frac{2 \varepsilon^2 B}{1 - \frac{B-1}{D_0}}\right). \end{aligned}$$

By construction, GPSL's depletion-aware sampling is exactly equivalent to drawing  $B$  points uniformly at random without replacement from the pooled dataset  $\mathcal{D}_0$ . Consequently, the class counts  $Y_m$  in GPSL follow the same hypergeometric law as in CL. Applying Serfling's inequality with finite-population correction and then a union bound over  $\mathcal{M}$  gives

$$\begin{aligned} \Pr\left(\Delta(\mathcal{B}, \boldsymbol{\beta}_0) \geq M \varepsilon\right) &= \sum_{m \in \mathcal{M}} \Pr\left(\left|\frac{Y_m}{B} - \beta_{0,m}\right| \geq \varepsilon\right) \\ &\leq 2M \exp\left(-\frac{2 \varepsilon^2 B}{1 - \frac{B-1}{D_0}}\right). \end{aligned}$$

Thus GPSL attains the exact same exponential-tail deviation guarantee (up to the standard finite-population factor) as centralized uniform sampling.

### C. Comparison with Fixed Local Batches

Under a scheme with a fixed local batch size as in [8], each client  $k$  contributes  $\tilde{B}_k = \lceil B \cdot \frac{D_k}{D_0} \rceil$  samples without replacement in each step. Defining  $\tilde{Y}'_m = \sum_{k \in \mathcal{K}} \tilde{Y}_{k,m}$  with

$$\tilde{Y}_{k,m} \sim \text{Hypergeometric}(D_k, c(D_k, m), \tilde{B}_k)$$

and  $\tilde{p}_m = \sum_{k \in \mathcal{K}} \frac{\tilde{B}_k}{B} \beta_{k,m}$  we decompose

$$\left|\frac{\tilde{Y}'_m}{B} - \beta_{0,m}\right| \leq \underbrace{\left|\frac{\tilde{Y}'_m}{B} - \tilde{p}_m\right|}_{\text{sampling noise}} + \underbrace{\left|\tilde{p}_m - \beta_{0,m}\right|}_{\text{rounding bias}}.$$

The sampling noise term still decays exponentially, but the rounding bias satisfies

$$\begin{aligned} \left|\tilde{p}_m - \beta_{0,m}\right| &= \left|\sum_{k \in \mathcal{K}} \left(\frac{\tilde{B}_k}{B} - \frac{D_k}{D_0}\right) \beta_{k,m}\right| \\ &\leq \sum_{k \in \mathcal{K}} \left|\frac{\tilde{B}_k}{B} - \frac{D_k}{D_0}\right| = \mathcal{O}\left(\frac{K}{B}\right) \end{aligned}$$

When  $K/B$  is large, the rounding bias can dominate and renders any exponential-tail guarantee ineffective. By contrast, GPSL's server-driven batch allocation incurs *zero* per-class rounding bias while retaining the same exponential decay. Fixed local batches may still perform adequately when  $K \ll B$  and rounding effects are negligible. However, such settings are rare in edge learning environments, where large  $K$  and small batch sizes dominate due to memory and communication constraints.

Moreover, the rounding exacerbates the issue of *client data depletion*, where client datasets are depleted disproportionately and faster. This increases the total number of training steps  $T$  and prolongs training. By contrast, GPSL prevents unnecessary inflation of  $T$  by keeping the global batch size  $B$  constant, regardless of the number of clients.

## V. SIMULATION RESULTS

In this section, we empirically evaluate the performance of GPSL compared to existing sampling methods in PSL. We examine the impact of sampling on batch deviation, training latency, and classification accuracy under both IID and non-IID data splits. We use the CIFAR10 dataset [23], which consists of 60,000 color images in  $M = 10$  classes. The dataset is split into  $D_0 = 50,000$  training and 10,000 test images. In all our experiments we trained a *ResNet18* [24] model for  $E = 100$  epochs using standard SGD. We chose the third layer of the ResNet18 model as the cut layer. For the client models we replaced BatchNorm [25] layers with GroupNorm [26] layers with a group size of 32. This is due to BatchNorm depending on the batch size and batch statistics, which is not compatible with GPSL, where the local batch sizes can vary. As optimizer we used the mini-batch SGD algorithm with momentum. We chose a learning rate of  $1 \times 10^{-2}$ , a momentum of 0.9 and  $\ell_2$  regularization with a weight decay of  $5 \times 10^{-4}$ . We chose the cross entropy loss function as objective.

### A. Sampling Methods

We compare GPSL against two sampling methods commonly used in PSL:

- **Fixed local sampling (FLS)** [15]: Each client  $k$  has the same local batch size  $B_k = \lceil B/K \rceil$ .
- **Fixed proportional sampling (FPLS)** [8]: Each client  $k$  has a proportional  $B_k \propto D_k$  with  $B_k = \lceil B \cdot \frac{D_k}{D_0} \rceil$ .

We also include a *centralized learning* (CL) baseline using random uniform sampling, where all data are pooled at the server and trained with a single model. This serves as an upper bound for performance.

In Table I we report the results of the sampling methods in the IID setting, where all clients have the same distribution. All sampling methods perform similarly, achieving near central learning performance.

### B. Non-IID Data

In the non-IID scenario, we employ a modified version of the extended Dirichlet allocation method proposed in [7], which ensures that each client receives data from exactly  $C$  classes. First,  $C$  distinct classes are assigned to each client using a multinomial-based allocation that promotes balanced class coverage across the client population. Then, for each class, a Dirichlet distribution with concentration parameter  $\alpha$  is sampled to determine how its samples are distributed among the clients assigned to it. Lower values of  $\alpha$  lead to more imbalanced allocations, where a class is concentrated heavily on one or a few clients. Higher values of  $\alpha$  result in more uniform class sample distributions across clients. By tuning  $C$  and  $\alpha$ , we can control the degree and structure of statistical heterogeneity across clients. We consider a *mild* non-IID scenario with  $C = 5$  and  $\alpha = 3.0$  and a *severe* non-IID scenario with  $C = 2$  and  $\alpha = 3.0$ . In Figure 2 we show an example of the data distribution for  $K = 16$  clients in the severe non-IID scenario.

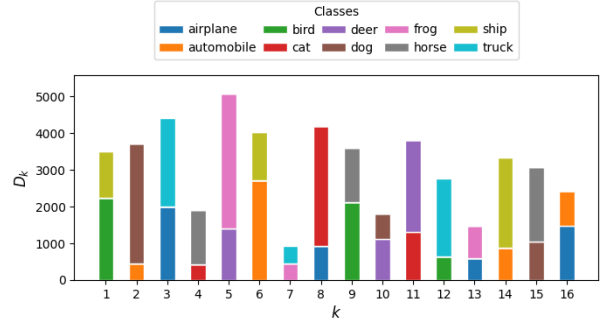


Fig. 2. Example of a severe non-IID setting for  $K = 16$  clients, showing the distribution of data across classes.

TABLE I  
IID TEST ACCURACY ON CIFAR10

Method	K = 16	K = 32	K = 64	K = 128
FLS	84.28 ± 0.22	84.38 ± 0.20	84.24 ± 0.41	84.17 ± 0.07
FPLS	84.28 ± 0.21	<b>84.48</b> ± 0.28	84.18 ± 0.86	<b>84.59</b> ± 0.76
GPSL	<b>84.37</b> ± 0.50	84.28 ± 0.38	<b>84.26</b> ± 0.33	84.35 ± 0.19

TABLE II  
SEVERE NON-IID TEST ACCURACY ON CIFAR10

Method	K = 16	K = 32	K = 64	K = 128
FLS	54.01 ± 16.84	53.56 ± 27.06	52.57 ± 26.13	58.88 ± 13.82
FPLS	49.14 ± 14.44	63.17 ± 5.38	64.35 ± 20.94	70.05 ± 12.25
GPSL	<b>84.37</b> ± 0.23	<b>84.43</b> ± 0.03	<b>84.71</b> ± 0.03	<b>84.31</b> ± 0.28

TABLE III  
MILD NON-IID TEST ACCURACY ON CIFAR10

Method	K = 16	K = 32	K = 64	K = 128
FLS	58.21 ± 10.19	65.54 ± 5.00	58.16 ± 23.66	65.09 ± 15.16
FPLS	67.73 ± 15.00	65.61 ± 11.29	63.41 ± 9.15	54.90 ± 19.62
GPSL	<b>84.50</b> ± 0.24	<b>84.22</b> ± 0.29	<b>84.30</b> ± 0.65	<b>84.21</b> ± 0.16

Top-1 test accuracy on CIFAR-10 under IID and non-IID settings for different numbers of clients  $K$  and global batch size  $B = 128$ . Each result is averaged over 5 random seeds and reported with standard deviation. CL achieved  $84.65 \pm 0.42$ . **Bold** values indicate the best result per column.

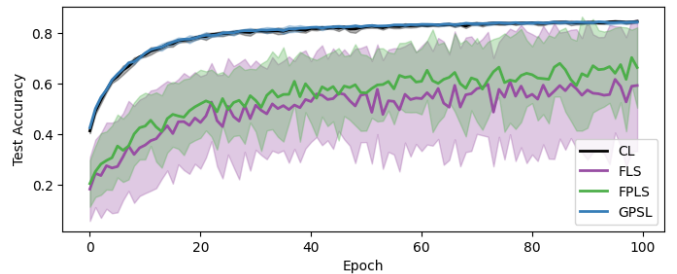


Fig. 3. Test accuracy curves for each sampling method over 5 runs with standard deviation shaded. Severe non-IID setting with  $K = 64$  clients and a global batch size of  $B = 128$ .

Table II shows the performance of each sampling method under severe non-IID conditions. Table III shows the per-

TABLE IV  
EFFECT OF GLOBAL BATCH SIZE ON SEVERE NON-IID TEST ACCURACY

Method	B = 64	B = 128	B = 256
FLS	60.11 ± 20.44	58.88 ± 13.82	41.94 ± 28.00
FPLS	58.39 ± 24.93	70.05 ± 12.25	58.96 ± 15.62
GPSL	<b>86.34</b> ± 0.19	84.31 ± 0.28	<b>81.94</b> ± 0.50
CL	85.35 ± 0.99	<b>84.65</b> ± 0.42	81.44 ± 0.73

Top-1 test accuracy on CIFAR-10 under severe non-IID settings for different global batch sizes  $B$ . Each result is averaged over 5 random seeds and reported with standard deviation.  $K = 128$  clients. **Bold** values indicate the best result per column.

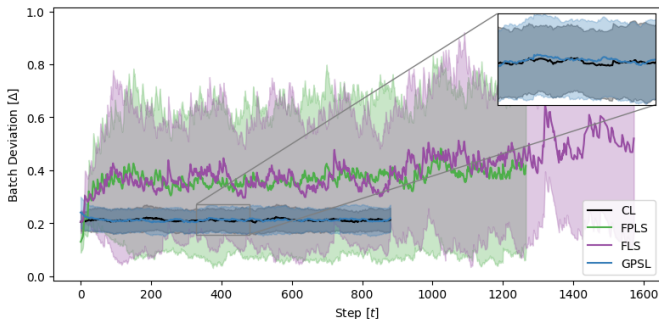


Fig. 4. Batch deviation curves for each sampling method over 5 runs with exponential moving average smoothing. Severe non-IID setting with  $K = 64$  clients and a global batch size of  $B = 128$ .

formance in a mild non-IID scenario. In both cases, GPSL achieves a test accuracy on par with centralized learning, while FPLS and FLS degrade significantly. The results are consistent across both mild and severe non-IID scenarios for varying client counts  $K$ , indicating scalability and robustness to the degree of data heterogeneity. Figure 3 shows the test accuracy curves for each sampling method under severe non-IID conditions. GPSL maintains a stable convergence curve, while FPLS and FLS exhibit significant fluctuations.

### C. Global Batch Size

Table IV shows performance results for the different sampling methods with varying batch sizes  $B$ . GPSL consistently outperforms FPLS and FLS across all batch sizes, demonstrating its robustness to batch size variations. In particular, GPSL enables flexibility in choosing the global batch size whereas FPLS and FLS are sensitive to the choice of batch size and may result in much larger global batch sizes than intended due to rounding and the client data depletion problem (Section IV-C).

### D. Batch Deviation

Figure 4 shows the empirical evaluation of the batch deviation as defined in Section IV-B for each sampling method under severe non-IID conditions. GPSL maintains a low and stable batch deviation almost matching CL, while FPLS and FLS exhibit significant fluctuations, particularly in the standard deviation. This aligns with our theoretical analysis and performance results, indicating that the batch deviation is the

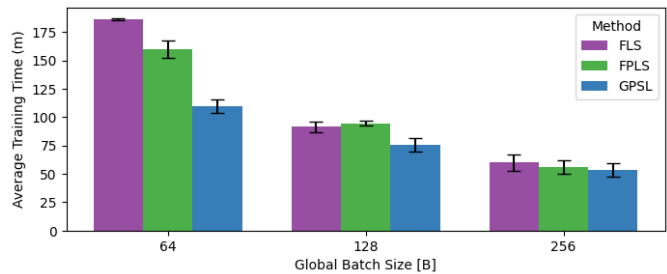


Fig. 5. Average total training time for each sampling method over 5 runs, measured in minutes. Severe non-IID setting with  $K = 64$  clients.

main reason for the performance degradation of FPLS and FLS.

Note that FLS and FPLS have more training steps than GPSL. This is due to the client data depletion problem, which leads to a larger number of batches per epoch with uneven batch sizes.

### E. Runtime

Figure 5 shows average training time for different global batch sizes  $B$ . GPSL consistently achieves a lower training time compared to FPLS and FLS. In particular when the global batch size is smaller. The computational overhead introduced by GPSL is thus negligible compared to the total training time saved. This result highlights that local sampling strategies can lead to a significant increase in the total training time due to the client data depletion problem. In particular, when the global batch size is smaller than the total number of clients.

### F. Limitations

While GPSL improves model performance and training efficiency, it inherits the PSL framework’s reliance on gradient averaging, which increases training latency and communication overhead. This limits its applicability to real-time and unstable IoT environments. Future work should explore integrating GPSL with client clustering [27] or communication-efficient techniques, such as adaptive compression [10], to improve scalability and reduce overhead.

## VI. CONCLUSION

We introduced parallel split learning with global sampling, a method designed to address the large effective batch size and non-independent and identically distributed data problems in distributed deep learning. By dynamically adjusting local batch sizes while maintaining a fixed global batch size, the method decouples the global batch size from the number of participating clients. Using standard concentration bounds, we showed that global sampling improves the alignment between global batches and the overall data distribution. Our simulation results confirm that the proposed method enhances convergence stability, boosts classification accuracy, and reduces training latency in non-independent and identically distributed scenarios. These findings suggest that server-driven global sampling offers a simple yet effective improvement for scalable distributed learning at the network edge.

## REFERENCES

- [1] J. Park, S. Samarakoon, M. Bennis, and M. Debbah, "Wireless Network Intelligence at the Edge," *Proc. IEEE*, vol. 107, no. 11, pp. 2204–2239, Nov. 2019. [Online]. Available: <https://ieeexplore.ieee.org/document/8865093/>
- [2] Z. Zhou, X. Chen, E. Li, L. Zeng, K. Luo, and J. Zhang, "Edge Intelligence: Paving the Last Mile of Artificial Intelligence With Edge Computing," *Proc. IEEE*, vol. 107, no. 8, pp. 1738–1762, Aug. 2019. [Online]. Available: <https://ieeexplore.ieee.org/document/8736011/>
- [3] J. Park, S. Wang, A. Elgabli, S. Oh, E. Jeong, H. Cha, H. Kim, S.-L. Kim, and M. Bennis, "Distilling On-Device Intelligence at the Network Edge," arXiv:1908.05895, Aug. 2019. [Online]. Available: <https://arxiv.org/pdf/1908.05895>
- [4] P. Vepakomma, O. Gupta, T. Swedish, and R. Raskar, "Split learning for health: Distributed deep learning without sharing raw patient data," arXiv:1812.00564, Dec. 2018. [Online]. Available: <https://www.semanticscholar.org/paper/Split-learning-for-health%3A-Distributed-deep-without-Vepakomma-Gupta/bbabd8a25260bf2413befcd756077efa81b1c618>
- [5] M. Poirot, P. Vepakomma, K. Chang, J. Kalpathy-Cramer, R. Gupta, and R. Raskar, "Split Learning for collaborative deep learning in healthcare," arXiv:1912.12115, Dec. 2019. [Online]. Available: <https://www.semanticscholar.org/paper/Split-Learning-for-collaborative-deep-learning-in-Poirot-Vepakomma/113e4c4ee777ce0cae57f3293a5c19a4c11dae13>
- [6] C. Thapa, M. A. P. Chamikara, and S. A. Camtepe, "Advancements of Federated Learning Towards Privacy Preservation: From Federated Learning to Split Learning," *Federated Learning Systems: Towards Next-Generation AI*, pp. 79–109, 2021. [Online]. Available: [https://link.springer.com/10.1007/978-3-030-70604-3\\_4](https://link.springer.com/10.1007/978-3-030-70604-3_4)
- [7] Y. Li and X. Lyu, "Convergence analysis of sequential federated learning on heterogeneous data," in *Proc. Int. Conf. on Neural Inf. Process. Syst.*, May 2024, pp. 56 700–56 755.
- [8] J. Jeon and J. Kim, "Privacy-Sensitive Parallel Split Learning," in *Int. Conf. on Inf. Netw.*, Jan. 2020, pp. 7–9. [Online]. Available: <https://ieeexplore.ieee.org/document/9016486>
- [9] W. Wu, M. Li, K. Qu, C. Zhou, X. Shen, W. Zhuang, X. Li, and W. Shi, "Split Learning Over Wireless Networks: Parallel Design and Resource Management," *IEEE J. Select. Areas Commun.*, vol. 41, no. 4, pp. 1051–1066, Apr. 2023. [Online]. Available: <https://ieeexplore.ieee.org/document/10040976/>
- [10] Z. Lin, G. Zhu, Y. Deng, X. Chen, Y. Gao, K. Huang, and Y. Fang, "Efficient Parallel Split Learning over Resource-constrained Wireless Edge Networks," arXiv:2303.15991, 2023. [Online]. Available: <https://arxiv.org/abs/2303.15991>
- [11] S. Oh, J. Park, P. Vepakomma, S. Baek, R. Raskar, M. Bennis, and S.-L. Kim, "LocFedMix-SL: Localize, Federate, and Mix for Improved Scalability, Convergence, and Latency in Split Learning," *Proc. of the ACM Web Conf.*, pp. 3347–3357, Apr. 2022. [Online]. Available: <https://dl.acm.org/doi/10.1145/3485447.3512153>
- [12] D.-J. Han, H. I. Bhatti, J. Lee, and J. Moon, "Accelerating Federated Learning with Split Learning on Locally Generated Losses," in *ICML Workshop on Federated Learn. for User Privacy and Data Confidentiality.*, Jul. 2021. [Online]. Available: <https://www.semanticscholar.org/paper/Accelerating-Federated-Learning-with-Split-Learning-Han-Bhatti/561ead22dfcae10f7590afedfac840e06670a96>
- [13] C. Thapa, P. C. Mahawaga Arachchige, S. Camtepe, and L. Sun, "SplitFed: When Federated Learning Meets Split Learning," *AAAI*, vol. 36, pp. 8485–8493, Jun. 2022. [Online]. Available: <https://ojs.aaai.org/index.php/AAAI/article/view/20825>
- [14] H. B. McMahan, E. Moore, D. Ramage, S. Hampson, and B. A. Y. Arcas, "Communication-Efficient Learning of Deep Networks from Decentralized Data," in *Proc. Int. Conf. Artif. Intell. and Statist.*, Apr. 2017, pp. 1273–1282. [Online]. Available: <https://www.semanticscholar.org/paper/Communication-Efficient-Learning-of-Deep-Networks-McMahan-Moore/d1dbf643447405984eeef098b1b320dee0b3b8a7>
- [15] S. Pal, M. Uniyal, J. Park, P. Vepakomma, R. Raskar, M. Bennis, M. Jeon, and J. Choi, "Server-Side Local Gradient Averaging and Learning Rate Acceleration for Scalable Split Learning," arXiv:2112.05929, Dec. 2021. [Online]. Available: <http://arxiv.org/abs/2112.05929>
- [16] "Mohkoh19/GPSL." [Online]. Available: <https://github.com/mohkoh19/GPSL>
- [17] X. Lyu, S. Liu, J. Liu, and C. Ren, "Scalable Aggregated Split Learning for Data-Driven Edge Intelligence on Internet-of-Things," *IEEE Internet of Things Magazine*, vol. 6, no. 4, pp. 124–129, Dec. 2023. [Online]. Available: <https://ieeexplore.ieee.org/document/10364651/>
- [18] N. Golmant, N. Vemuri, Z. Yao, V. Feinberg, A. Gholami, K. Rothauge, M. W. Mahoney, and J. E. Gonzalez, "On the Computational Inefficiency of Large Batch Sizes for Stochastic Gradient Descent," arXiv:1811.12941, Sep. 2018. [Online]. Available: <https://www.semanticscholar.org/paper/On-the-Computational-Inefficiency-of-Large-Batch-Golmant-Vemuri/3fd9e04da135496bcd75e884b5cd2ecee656a67d>
- [19] D. Wilson and T. R. Martinez, "The general inefficiency of batch training for gradient descent learning," *Neural Networks*, vol. 16, no. 10, pp. 1429–1451, Dec. 2003. [Online]. Available: <https://linkinghub.elsevier.com/retrieve/pii/S0893608003001382>
- [20] Y. Cai and T. Wei, "Efficient Split Learning with Non-iid Data," in *IEEE Int. Conf. on Mobile Data Manage.*, Jun. 2022, pp. 128–136. [Online]. Available: <https://ieeexplore.ieee.org/document/9861117>
- [21] M. Kim, A. DeRieux, and W. Saad, "A Bargaining Game for Personalized, Energy Efficient Split Learning over Wireless Networks," in *IEEE Wireless Commun. and Netw. Conf.* Glasgow, United Kingdom: IEEE, Mar. 2023, pp. 1–6. [Online]. Available: <https://ieeexplore.ieee.org/document/10118601/>
- [22] R. J. Serfling, "Probability inequalities for the sum in sampling without replacement," *Ann. Statist.*, vol. 2, no. 1, pp. 39–48, Jan. 1974.
- [23] A. Krizhevsky, "Learning Multiple Layers of Features from Tiny Images," University of Toronto, Technical Report, 2009. [Online]. Available: <https://www.semanticscholar.org/paper/Learning-Multiple-Layers-of-Features-from-Tiny-Krizhevsky/5d90f06bb70a0a3dced62413346235c02b1aa086>
- [24] K. He, X. Zhang, S. Ren, and J. Sun, "Deep Residual Learning for Image Recognition," in *Proc. IEEE Conf. on Comput. Vis. and Pattern Recognit.*, 2016, pp. 770–778. [Online]. Available: <http://ieeexplore.ieee.org/document/7780459/>
- [25] S. Ioffe and C. Szegedy, "Batch Normalization: Accelerating Deep Network Training by Reducing Internal Covariate Shift," in *Int. Conf. on Mach. Learn.*, Feb. 2015, pp. 448–456. [Online]. Available: <https://www.semanticscholar.org/paper/Batch-Normalization%3A-Accelerating-Deep-Network-by-Ioffe-Szegedy/995c5f5e62614fcb4d2796ad2faab969da51713e>
- [26] Y. Wu and K. He, "Group Normalization," *Int. J. Comput. Vis.*, vol. 128, no. 3, pp. 742–755, Mar. 2020. [Online]. Available: <http://link.springer.com/10.1007/s11263-019-01198-w>
- [27] X. Liu, Y. Deng, and T. Mahmoodi, "Wireless Distributed Learning: A New Hybrid Split and Federated Learning Approach," *IEEE Trans. Wireless Commun.*, vol. 22, no. 4, pp. 2650–2665, Apr. 2023. [Online]. Available: <https://ieeexplore.ieee.org/document/9923620/>